Supplemental Information

Exosome secretion is enhanced by invadopodia and drives invasive behavior.

Daisuke Hoshino, Kellye C. Kirkbride, Kaitlin Costello, Emily S. Clark, Seema Sinha, Nathan Grega-Larson, Matthew J. Tyska, and Alissa M. Weaver

Figure S1

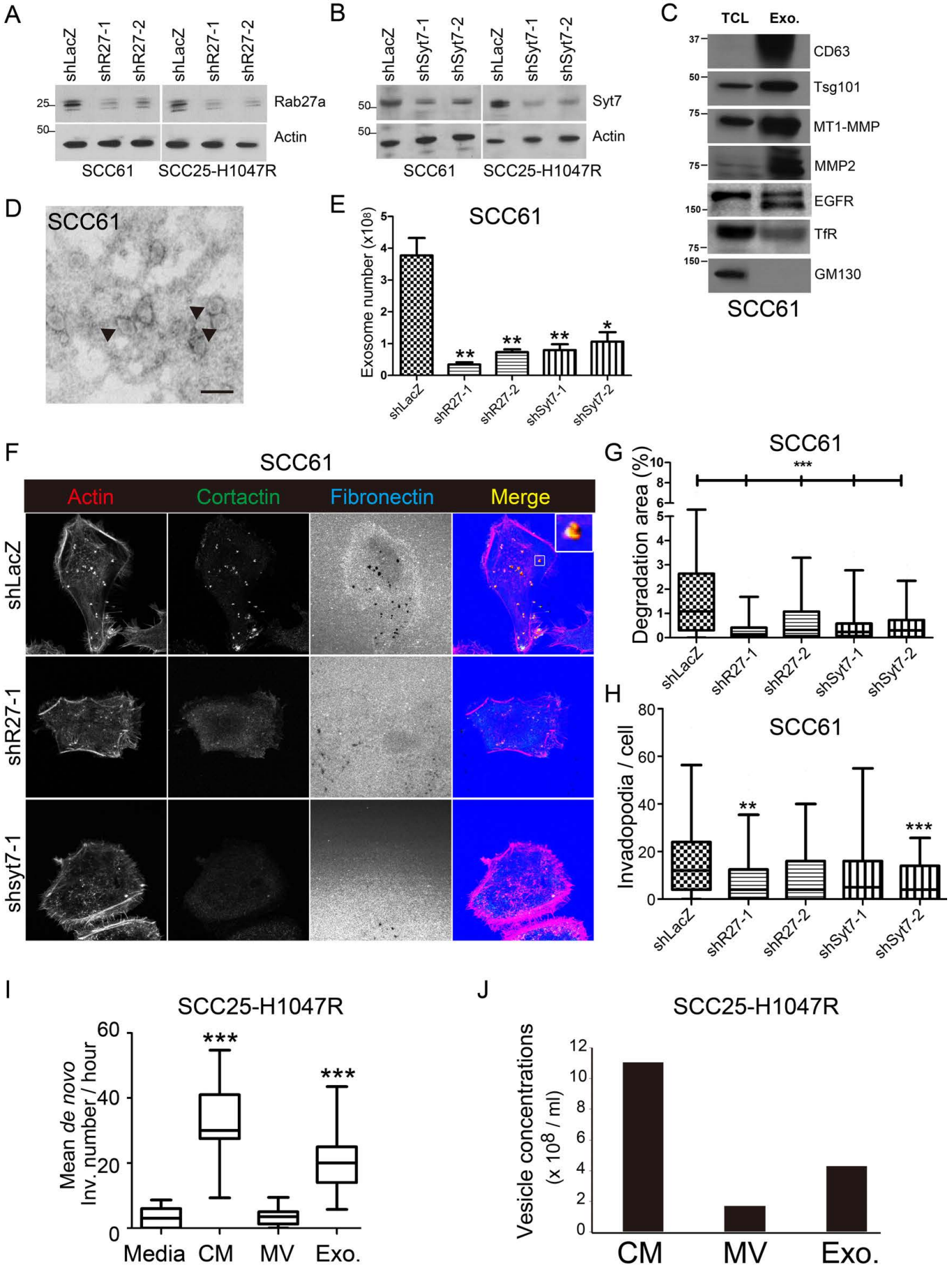
A
shLacZ
shR27-1
shR27-2
shLacZ
shR27-1
shR27-2
25
50
Rab27a
Actin
SCC61
SCC25-H1047R
B
shLacZ
shSyt7-1
shSyt7-2
shLacZ
shSyt7-1
shSyt7-2
50
50
Syt7
Actin
SCC61
SCC25-H1047R
C
TCL
Exo.
37
50
75
75
150
75
150
CD63
Tsg101
MT1-MMP
MMP2
EGFR
TfR
GM130
SCC61
D
SCC61
E
SCC61
Exosome number (x10⁸)
0
1
2
3
4
5
**
**
**
*
shLacZ
shR27-1
shR27-2
shSyt7-1
shSyt7-2
F
SCC61
Actin
Cortactin
Fibronectin
Merge
shLacZ
shR27-1
shsyt7-1
G
SCC61
***
Degradation area (%)
0
1
2
3
4
5
6
8
10
shLacZ
shR27-1
shR27-2
shSyt7-1
shSyt7-2
H
SCC61
Invadopodia / cell
0
20
40
60
80
**
***
shLacZ
shR27-1
shR27-2
shSyt7-1
shSyt7-2
I
SCC25-H1047R
Mean de novo Inv. number / hour
0
20
40
60
***
***
Media
CM
MV
Exo.
J
SCC25-H1047R
Vesicle concentrations (x 10⁸ / ml)
0
2
4
6
8
10
12
CM
MV
Exo.

Figure S2

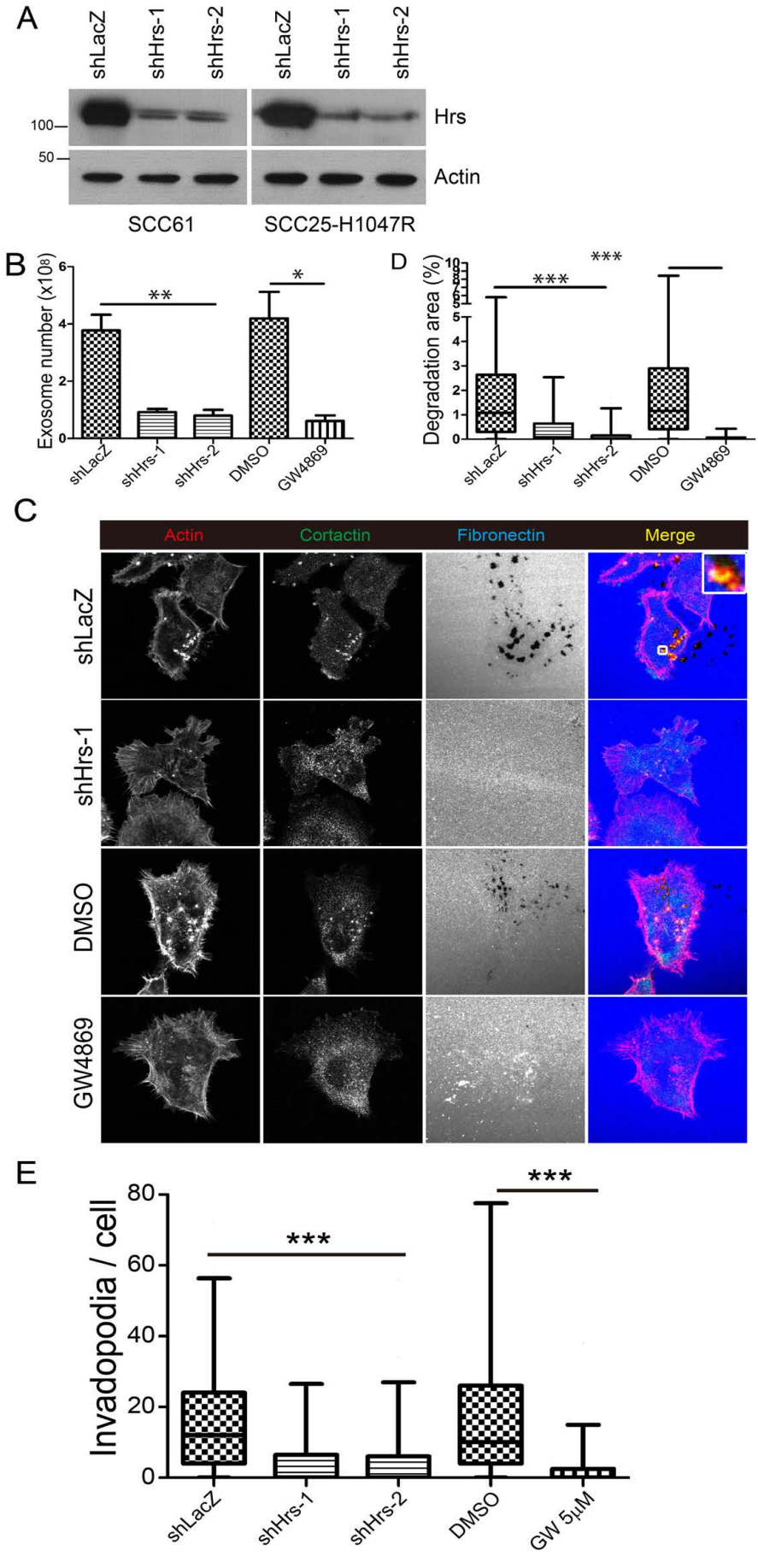
A
shLacZ
shHrs-1
shHrs-2
shLacZ
shHrs-1
shHrs-2
100
50
Hrs
Actin
SCC61
SCC25-H1047R
B
Exosome number (x10⁸)
**
*
shLacZ
shHrs-1
shHrs-2
DMSO
GW4869
D
Degradation area (%)
***
***
shLacZ
shHrs-1
shHrs-2
DMSO
GW4869
C
Actin
Cortactin
Fibronectin
Merge
shLacZ
shHrs-1
DMSO
GW4869
E
Invadopodia / cell
***
***
shLacZ
shHrs-1
shHrs-2
DMSO
GW 5μM

Figure S3

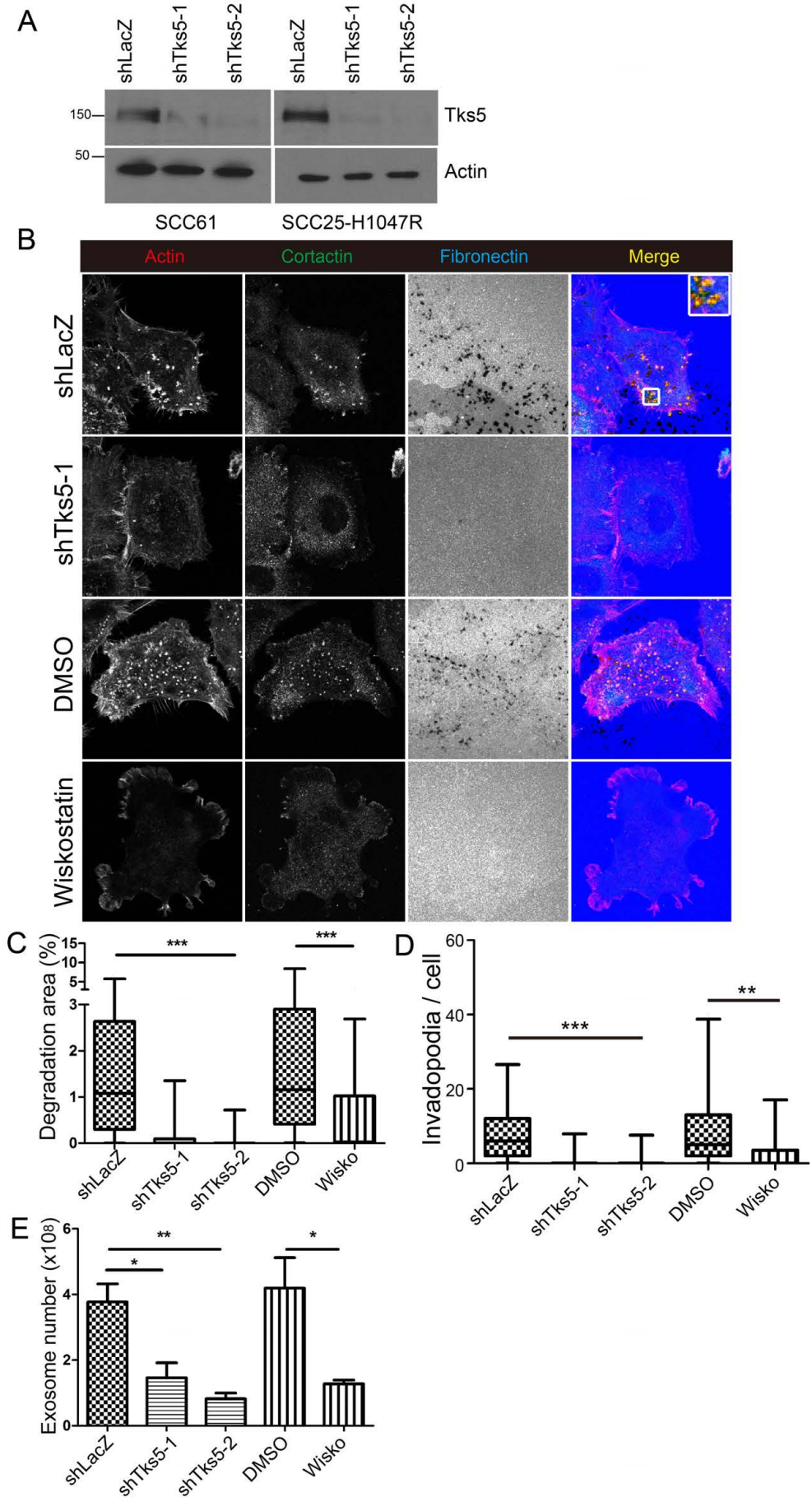
A
shLacZ
shTks5-1
shTks5-2
shLacZ
shTks5-1
shTks5-2
150
50
Tks5
Actin
SCC61
SCC25-H1047R
B
Actin
Cortactin
Fibronectin
Merge
shLacZ
shTks5-1
DMSO
Wiskostatin
C
Degradation area (%)
***
***
shLacZ
shTks5-1
shTks5-2
DMSO
Wisko
D
Invadopodia / cell
***
**
shLacZ
shTks5-1
shTks5-2
DMSO
Wisko
E
Exosome number (x10⁸)
**
*
*
shLacZ
shTks5-1
shTks5-2
DMSO
Wisko

Figure S4.

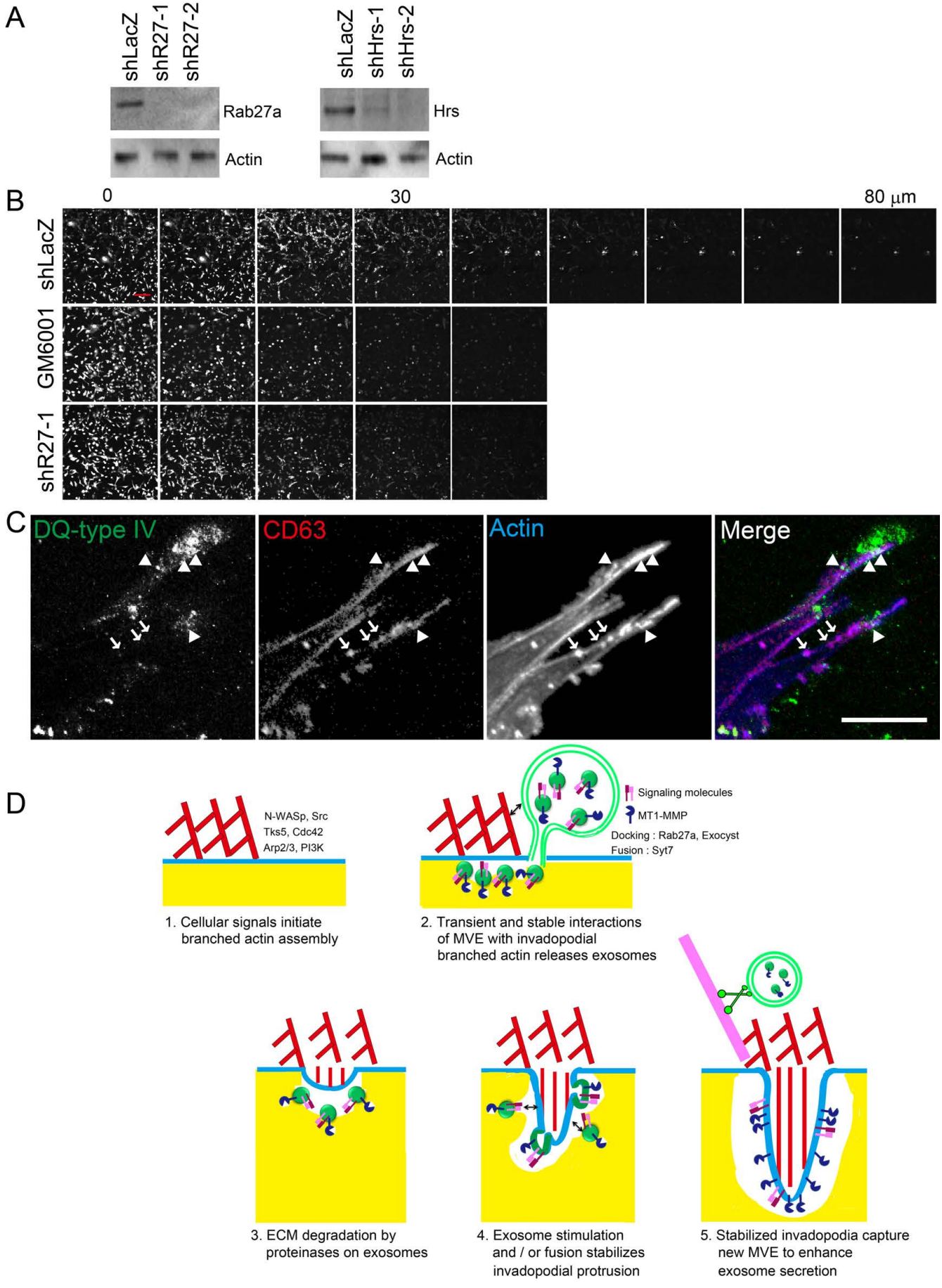
A
shLacZ
shR27-1
shR27-2
Rab27a
Actin
shLacZ
shHrs-1
shHrs-2
Hrs
Actin
B
0
30
80 μm
shLacZ
GM6001
shR27-1
C
DQ-type IV
CD63
Actin
Merge
D
N-WASp, Src
Tks5, Cdc42
Arp2/3, PI3K
1. Cellular signals initiate branched actin assembly
Signaling molecules
MT1-MMP
Docking : Rab27a, Exocyst
Fusion : Syt7
2. Transient and stable interactions of MVE with invadopodial branched actin releases exosomes
3. ECM degradation by proteinases on exosomes
4. Exosome stimulation and / or fusion stabilizes invadopodial protrusion
5. Stabilized invadopodia capture new MVE to enhance exosome secretion

SUPPLEMENTARY FIGURE LEGENDS

Figure S1. Exosome Secretion Promotes Invadopodia Formation And Maturation In SCC61 Cells, Related To Figure 2. Western blot analysis of (A) Rab27a ("shR27-1 or -2") or (B) Synaptotagmin-7 (Syt) knockdown efficiency in SCC61, SCC25-H1047R cells, compared with shLacZ control; (C) Western blots, illustrating the presence of CD63, Tsg101, MMP2, MT1-MMP, EGFR and Transferrin receptor (TfR) in SCC61 total cell lysates (TCL) and exosomes (Exo.). Note that there is no detectable contamination of exosomes by GM130 (Golgi). (D) Exosomes purified from cell culture supernatants were negatively stained and analysed by electron microscopy. Arrowheads indicate exosomes. Scale bar, 100 nm. (E) Quantification of exosome numbers from cell culture supernatants by NanoSight nanoparticle tracking analysis from 3 independent experiments. Mean +/-SEM. (F) Images of SCC61 cells control cells (shLacZ) and Rab27a knockdown cells (shR27-1) cultured on fibronectin (blue) coated gelatin plates and immunostained for cortactin (green) and F-actin (red). Scale bars=20 μm. n > 52 cells per cell line from 3 independent experiments. (G) Quantification of invadopodia mediated ECM degradation (% cell area). (H) Quantification of invadopodia number per cell. (I) SCC25-H1047R shLacZ expressing F-tractin were cultured on FN-coated gelatin plates without growth factors for 24 hrs before the addition of 1 ml each of OPTI-MEM (Media), conditioned medium (CM), microvesicles (MV), or exosome (Exo) fractions mixed with L15 medium 1 : 1. After 1 h, live movies were obtained every 1 min for 1h. (J) Quantification of vesicle number in each resuspended fraction by NanoSight. See Supplementary Experimental Procedures for further details about the purification and resuspension procedure. Data are plotted as box-and-whiskers plots where the median is represented with a line, the box represents the 25-75 percentile, and the error bars show the 5-95 percentile. * $p<0.05$, **, $p<0.01$, ***$p<0.001$

Figure S2. Exosome Biogenesis Controls Invadopodia Activity In SCC61 Cells, Related To Figure 3. (A) Western blot analysis of Hrs-knockdown efficiency in SCC61, SCC25-H1047R cells. (B) Quantification of exosome numbers. N = 3 independent experiments. (C) Images of SCC61 control (shLacZ), Hrs knockdown (shHrs-1), DMSO- and GW4869 (GW) treated cells cultured on fibronectin (blue)-coated gelatin plates and immunostained for cortactin (green) and F-actin (red). Scale bars 20=μm. n > 50 cells per condition from 3 independent experiments. (D) Quantification of invadopodia-associated ECM degradation (% cell area). (E) Quantification of invadopodia number per cell. Data are plotted as box-and-whiskers plots where the median is represented with a line, the box represents the 25-75 percentile, and the error bars show the 5-95 percentile. Control shLacZ data for B,D,E are the same as Fig S1E,G. * $p<0.05$, **, $p<0.01$, ***$p<0.001$

Figure S3. Invadopodia Docking Sites Significantly Contribute To The Secretion Of Exosomes In SCC61 Cells, Related To Figure 4. (A) Western blot analysis of Tks5 knockdown efficiency in SCC61 and SCC25-H1047R cells. (B) Images of SCC61 control (shLacZ), Tks5 knockdown (shTks5-1), DMSO- or Wiskostatin treated cells cultured on fibronectin (blue)-coated gelatin plates and immunostained for cortactin (green) and F-actin (red). Scale bars=20 μm. n > 44 cells per cell line from 3 independent experiments. (C) Quantification of invadopodia-associated ECM degradation (% cell area). (D) Quantification of invadopodia number per cell. Data are plotted as box-and-whiskers plots where the median is represented with a line, the box represents the 25-75 percentile, and the error bars show the 5-95 percentile. (E) Quantification of exosome numbers. n=3 independent experiments. Mean +/-SEM. Control shLacZ and DMSO data for C,D,E are the same as Fig S1E,G and S2 B,D,E, respectively. * $p<0.05$, **, $p<0.01$, ***$p<0.001$

Figure S4. Images from Inverted Invasion and Invadopodia Assay for MDA-MB-231 cells and Model, Related to Figure 4.
(A) Western blot analysis of Rab27a-KD efficiency in MDA-MB-231 cells. (B) Serial optical sections from cells invaded into Matrigel in the inverted invasion assay were captured at 10 μm intervals and presented as a representative sequence in which the individual optical sections are placed alongside one another, with increasing depth from left to right as indicated. 0 μm indicates cells that crawled through the filter but did not enter the gel. Scale bar, 200 μm. (C) Images of MDA-MB-231 cells cultured in 3D matrigel containing DQ-type IV collagen stained for CD63 (Red) and F-actin (Blue). The green signal shows degraded type IV collagen. Arrowheads indicate type IV collagen degradation associated with CD63- and actin-positive protrusion tips whereas arrows indicate more centrally located CD63-positive vesicular-appearing puncta without associated collagen degradation. Scale bar, 20 μm. (D) Model of exosome-invadopodia synergistic interactions. 1. Local activation of cellular signals induces branched actin assembly to initiate invadopodia

formation. 2. Branched actin-associated docking and tethering factors (double-headed arrow) such as the Exocyst complex facilitate transient and stable interactions of multivesicular endosomes (MVE) with invadopodia, leading to secretion of exosomes. 3. Proteinases on secreted exosomes degrade ECM to allow space for protrusion. 4. Exosome stimulation and/or fusion with the nascent protrusion adds membrane and signaling molecules to stabilize invadopodia. 5. Stabilized invadopodia with robust signaling captures more MVE to enhance exosome secretion and induce the formation of additional invadopodia.

SUPPLEMENTARY MOVIES

Movie S1, Related to Figure 1. SCC25-H1047R cells stably expressing tdTomato-F-Tractin (red) were transfected with GFP-CD63 (green) and cultured on fibronectin-coated gelatin. Confocal images were captured every 0.97 sec for 5 min. Arrowheads indicate examples of invadopodia that interact with GFP-CD63-positive endosomes.

Movies S2 and S3, Related to Figure 1. SCC25-H1047R cells stably expressing tdTomato-F-Tractin (red) were transfected with GFP-CD63 (green) and cultured on fibronectin-coated dishes. TIRF images were captured every 2.8 sec for 5 min. Arrowheads indicate examples of invadopodia that interact with GFP-CD63-positive endosomes. Note both transient (Movie S2) and stable (Movie S3) interactions of MVE with invadopodia.

Movie S4, Related to Figure 2. SCC25-H1047R cells stably expressing tdTomato-F-Tractin (red) were serum starved and then stimulated with GFP-CD63-positive exosomes (green, Right panel). Red puncta are invadopodia. Images were captured every 2min for 4 hrs.

SUPPLEMENTAL EXPERIMENTAL PROCEDURES

Cell lines

Cells were cultured in DMEM supplemented with 20% FBS and 0.4 mg/ml hydrocortisone (SCC61, SCC25, SCC25-1047) or 10% FBS (MDA-MB-231).

Plasmids and Reagents.

tdTomato–F-tractin-pLenti6 vector was previously described (Hoshino et al., 2012). GFP-CD63 was a gift of Dr. Gillian Griffiths (Cambridge Institute for Medical Research, Cambridge, UK) and subcloned into pLenti6 vector. GFP-Rab27a was a gift of Dr. Nikolai Kiskin (MRC National Institute for Medical Research, London, UK). MT1-MMP-pHLuorin-pLenti6 vector was previously described (Branch et al., 2012). shRNAs: Rab27a-1: 5′- gtgcgatcaaatggtcatgcc -3′, Rab27a-2: 5′- cgttcttcagagatgctatgc -3′, Syt7-1: 5′- gaacgagaccttcctctttgc -3′, Syt7-2: 5′- caatgacgtcatcggcaagac -3′, Hrs-1: 5′- gacctgctgaagagacaagtc -3′, Hrs-2: 5′- gcatgaagagtaaccacagc -3′, Tks5-1: 5′- gtctctcccttggcgtatatc -3′, Tks5-2: 5′- cagttcctttgcatgtttcgc -3′. shRNAs were cloned into pLenti6/ Block iT^{TM}. Wiskostatin (Calbiochem) and GW4869 (Sigma) were tested at multiple concentrations within the range previously found to be effective and with minimal off-target effects or toxicity (Kosaka et al., 2010; Peterson et al., 2004).

Invadopodia assay

Glass-bottom poly-D-lysine–coated dishes (35 mm; MatTek) were coated with 2.5% bovine gelatin. The gelatin was cross-linked with a 0.5% glutaraldehyde solution, followed by quenching with sodium borohydride (1 mg/ml) and incubation with DyLight633-labeled fibronectin for 1 hour for SCC25-H1047R and SCC61 cells. For MDA-MB-231 cells, FITC-gelatin was cross-linked and used. Cells (8×10^4) were seeded to each plate containing 2 ml of invadopodia medium (DMEM, 5% NuSerum, 10% FBS, EGF (100 ng/ml)). After 18 hours, cells were fixed with 4% paraformaldehyde (PFA), permeabilized with 0.1% Triton X-100, blocked with 5% bovine serum albumin (BSA), and probed for cortactin (Millipore, 4F11 mAb) and F-actin (Rhodamine phalloidin and Alexa 633 phalloidin, Invitrogen).

Microscopy and image analysis

Confocal images were obtained with a Zeiss LSM 510 and LSM 710 (both 63X PlanApo objectives). TIRF microscopy was performed on a Nikon TiE inverted light microscope equipped with a Nikon TIRF illuminator, a ×100/1.49 numerical aperture TIRF objective (used in combination with a ×1.5 optivar), a Hamamatsu Imag

EM-CCD camera or Roper Evolve EM-CCD. Wide-field movies were obtained on a Nikon Eclipse TE2000E microscope equipped with a 37℃ chamber and a cooled charge-coupled device (CCD) camera (Hamamatsu ORCA-ER).

Live cell imaging conditions
For confocal live cell imaging, SCC25-H1047R cells stably expressing tdTomato-F-Tractin were transfected with GFP-CD63 or GFP-Rab27a then cultured on gelatin-fibronectin–coated dishes. After 24 hours, images were captured every 0.97 s for 5 min. For TIRF live cell imaging, SCC25-H1047R cells stably expressing tdTomato-F-Tractin were transfected with GFP-CD63 or GFP-Rab27a cultured on fibronectin–coated dishes. After 24 hours, images were captured every 2.8 s for 5 min.
For invadopodia formation and lifetime analyses (basal condition), SCC25-H1047R-shLacZ and –shR27 cells stably expressing tdTomato–F-tractin cultured on gelatin-fibronectin–coated dishes. After 24 hours, images were captured by wide-field epifluorescence microscopy every 90 s for 90min. For exosome stimulation analyses, SCC25-H1047R cells stably expressing tdTomato–F-tractin were cultured on gelatin-fibronectin–coated dishes. After 24 hours, for the growth factor-free condition, the media was replaced with serum-free medium for 24 hours before addition of 2 x 10^6 exosomes derived from SCC25-H1047R stably expressing GFP-CD63. For the growth factor-replete condition, exosomes or buffer were simply added into the invadopodia formation medium. 1 h after addition of the exosomes, images were captured every 2 min for 4 hrs.

MDA-MB-231 3D movies
5 x 10^4 cells in 100 µl growth medium were embedded in Matrigel (BD) and mixed gently before plating in a 35 mm Mat-tek dish and incubating at 37°C for 2 h. Then, medium supplemented with 10% FBS and 100 ng/ml EGF was added on top of the Matrigel. After 24 h, images were captured in 2.5 µm slices for a total of 19 z-slices gathered every 21 s for 17.5 min.

MDA-MB-231 3D DQ-type IV collagen assay
5 x 10^4 cells were embedded in 250 µl of Matrigel containing 25 µg/ml DQ-type IV collagen (Invitrogen) and mixed gently before plating in a 35 mm Mat-tek dish and incubating at 37°C for 2 h. Then, medium supplemented with 10% FBS and 100 ng/ml EGF was added on top of the Matrigel. After 72 hrs, cells were fixed with 4% paraformaldehyde (PFA), permeabilized with 0.5% saponin, blocked with 5% bovine serum albumin (BSA), and probed for CD63 (Abcam, MEM259 mAb) and F-actin (Alexa 633 phalloidin, Invitrogen).

Invadopodia analyses on fixed immunostained cells.
Invadopodia were manually counted as actin-positive puncta that colocalized with extracellular matrix degradation. Matrix degradation was quantitated from the fluorescent fibronectin images in MetaMorph software with the threshold tool to obtain an inclusive threshold of the dark holes in the matrix, followed by analysis of the threshold area with the “Region Measurements” tool. Degradation area per cell area was plotted.

Invasion assays
Inverted invasion assays were performed as described previously (Yu et al., 2012). In brief, Matrigel (BD) was diluted with PBS in 1:1 volume and polymerized in transwell inserts (Corning) at 37°C for at least 1 h. Inserts were then inverted, and 5 × 10^4 cells were seeded directly onto the outside surface of the filter. Serum-free medium was finally added to transwell inserts, and medium supplemented with 10% FBS and 100 ng/ml EGF was added atop the Matrigel. Invading cells were stained with Hoechst at 72 h after seeding. Cells failing to cross the filter were removed with tissue, and confocal microscopy was used to visualize cells that crossed through the filter. Serial optical sections were captured at 10 µm intervals. The relative index of invasion was calculated as the fluorescence intensity of cells that had invaded beyond 30 µm compared to control cells.

Exosome collection
80% confluent plates of cells were rinsed with PBS twice and incubated with OPTI-MEM for 30 min before changing the media to fresh OPTI-MEM and incubation for 48 hrs. Conditioned media were collected and the final cell number was counted by hemocytometer. Exosomes were isolated from conditioned medium using sequential centrifugation at 4 °C, with 15 min at 2000x*g* to remove cell debris, and 3 hrs at 100,000x*g* to

pellet exosomes. The pellet was then re-suspended in PBS and recentrifuged for 3 hrs at 100,000x*g* to obtain purified exosomes. The purified exosome pellet was resuspended in PBS and adjusted according to the final cell number count to yield equivalent secreted exosome concentrations on a per cell basis. Exosomes were then counted by NanoSight nanoparticle tracking analysis (NanoSight, Ltd., Amesbury, UK).

Microvesicle collection for live imaging.
80% confluent plates of cells were rinsed twice with PBS and incubated with 15ml of OPTI-MEM for 30 min before changing the media to fresh 15 ml of OPTI-MEM and incubation for 48 hrs. Conditioned media were collected and sequentially centrifuged at 4 °C, with 15 min at 2000x*g* to remove cell debris (this fraction was used as CM in Figures S1I and S1J), and at 2 hrs at 16,000 x*g* to pellet microvesicles (this pellet was re-suspended in 15ml of OPTI-MEM and used as the microvesicles fraction, MV, in Figures S1I and S1J). The supernatant from the microvesicle pellet was then centrifuged at 2 hrs at 100,000 x*g* to pellet exosomes and was re-suspended in 15ml of OPTI-MEM to obtain the exosomes fraction, Exo, for the experiment in Figures S1I and S1J.

Electron Microscopy
SCC61 Cells were cultured overnight on transwell filters (6.5-mm, 8.0-μm pore size; Fisher Scientific, Pittsburgh, PA) coated with 2.5% gelatin. The transwell membrane was removed, fixed in 2.5% glutaraldehyde in 0.1 M cacodylate buffer, stained in 1% osmium tetraoxide, dehydrated in successive alcohol incubations, and embedded in Spurr's resin overnight. Sections (100 nm) were cut, with the cells remaining on the transwells to ensure proper orientation. Electron microscopy was performed using a Philips CM-12 functioning at 80 keV.

Preparation of negatively stained grids for electron microscopy
Formvar carbon film-coated grids (FCF-200-Cu; Electron Microscopy Sciences; Hatfield, PA) were washed in double distilled water, followed by 100% ethanol. For each step, excess liquid was removed by wicking with filter paper. The sample (5 ml) was added to the grid for 60s. The exosome preparation from SCC61 cells was diluted 1:100 prior to adding to the grid, while the SCC25 H1047R exosome preparation samples were used directly. Grids were immediately stained with 2% phosphotungstic acid, pH 6.1 for 15s and allowed to dry overnight. Grids were imaged using a FEI Tecnai T12 TEM (120 kV LaB6 source), Gatan cryotransfer stage, and AMT XR41-S side mounted 2K X 2K CCD camera, 2102 SC. All exosome images were captured at a magnification of 53,000x.

SUPPLEMENTAL REFERENCES

Branch, K.M., Hoshino, D., and Weaver, A.M. (2012). Adhesion rings surround invadopodia and promote maturation. Biology Open *1*, 711-722.
Hoshino, D., Jourquin, J., Emmons, S.W., Miller, T., Goldgof, M., Costello, K., Tyson, D.R., Brown, B., Lu, Y., Prasad, N.K.*, et al.* (2012). Network analysis of the focal adhesion to invadopodia transition identifies a PI3K-PKCalpha invasive signaling axis. Sci Signal *5*, ra66.
Kosaka, N., Iguchi, H., Yoshioka, Y., Takeshita, F., Matsuki, Y., and Ochiya, T. (2010). Secretory mechanisms and intercellular transfer of microRNAs in living cells. J Biol Chem *285*, 17442-17452.
Peterson, J.R., Bickford, L.C., Morgan, D., Kim, A.S., Ouerfelli, O., Kirschner, M.W., and Rosen, M.K. (2004). Chemical inhibition of N-WASP by stabilization of a native autoinhibited conformation. Nat Struct Mol Biol *11*, 747-755.
Yu, X., Zech, T., McDonald, L., Gonzalez, E.G., Li, A., Macpherson, I., Schwarz, J.P., Spence, H., Futo, K., Timpson, P.*, et al.* (2012). N-WASP coordinates the delivery and F-actin-mediated capture of MT1-MMP at invasive pseudopods. J Cell Biol *199*, 527-544.